Bioresource Technology 309 (2020) 123402

Contents lists available at ScienceDirect

Bioresource Technology

journal homepage: www.elsevier.com/locate/biortech

Dual detection of biochemical oxygen demand and nitrate in water based on bidirectional *Shewanella loihica* electron transfer

Yue Yi[a,b,c], Ting Zhao[a,b,c], Beizhen Xie[a,b,c], Yuxuan Zang[a,b,c], Hong Liu[a,b,c,*]

[a] Beijing Advanced Innovation Center for Biomedical Engineering, Beihang University, Beijing 100083, China
[b] Institute of Environmental Biology and Life Support Technology, School of Biological Science and Medical Engineering, Beihang University, Beijing 100083, China
[c] International Joint Research Center of Aerospace Biotechnology & Medical Engineering, Beihang University, Beijing 100191, China

GRAPHICAL ABSTRACT

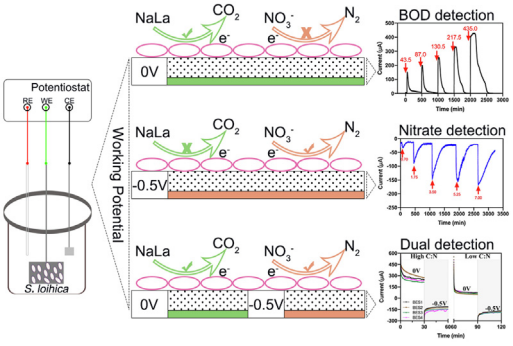

ARTICLE INFO

Keywords:
BOD detection
Nitrate detection
Biosensor
Bioelectrochemical system
Bidirectional extracellular electron transfer

ABSTRACT

This study for the first time proposed a method for simultaneously measuring BOD and nitrate in water using electrochemically active bacteria. Firstly, the bidirectional extracellular electron transfer (EET) capability of a model electricigen *Shewanella loihica* PV-4 was revealed. Then, based on the respective outward and inward EET, *S. loihica* PV-4 was utilized to detection BOD and nitrate. The results demonstrated a positive correlation between the outward EET and BOD (from 0 mg/L to 435 mg/L) while a negative correlation between the inward EET and nitrate (from 0 mg/L to 7 mg/L); both the relationships were well fitted by the combination of traditional linear model and Michaelis-Menten model ($R^2 > 0.96$). Finally, a dual detection method for BOD and nitrate measurements was established based on the ano-cathodophilic capability of *S. loihica* PV-4 biofilm, and exhibited the characteristics of high accuracy (> 80%) and fast analysis (< 1 h), suggesting a promising prospect in water monitoring.

1. Introduction

Water pollution is a severe environmental issue threatening ecological security and public health. Water quality monitoring, *i.e.* measuring and tracking the key indicators of water, has been proved to be efficient for water pollution prevention. Among these indicators, biochemical oxygen demand (BOD), which reflects the content of the biodegradable organic pollutants in water, is considered to be an essential index for the estimation of organic contamination (Jouanneau et al., 2014). Excessive BOD in water may lead to an explosion of

* Corresponding author at: School of Biological Science and Medical Engineering, Beihang University, 37 Xueyuan RD, Haidian DIST, Beijing 100083, China.
E-mail address: LH64@buaa.edu.cn (H. Liu).

https://doi.org/10.1016/j.biortech.2020.123402
Received 22 February 2020; Received in revised form 15 April 2020; Accepted 16 April 2020
Available online 18 April 2020
0960-8524/

aerobic microorganisms, which will deplete limited dissolved oxygen, and eventually result in the massive death of fish and water quality deterioration. Besides, eutrophication and algal bloom in aquatic ecosystems have also drawn growing concern worldwide (Hu and Ren, 2019), and the primary reason is the excessive discharge of nitrate induced by the misuse of fertilizers and food additives (Carey et al., 2016). Therefore, it is of great significance to develop the real-time and on-line detection methods for BOD and nitrate in water.

According to the standard method of BOD measurement, BOD is determined by measuring the oxygen consumption of the aerobic biochemical reaction in water within a certain period (usually 5 days); thus, the test result is obviously lagging behind the real-time water quality, and the method is not suitable for on-line and in-situ monitoring. Another alternative method is the biosensors based on immobilized microorganisms; this method can achieve a rapid BOD measurement, but the electrical signals of the immobilized microorganisms are relatively weak and are easy to be interfered (Liu et al., 2015; Zaitseva et al., 2017). Moreover, the maintenance cost is relatively high due to the consumption of immobilized bio-electrode during detection process. Compared with BOD measurements, nitrate detection needs higher specificity and more complicated technologies. Conventional methods, including phenol disulfonic acid spectrophotometry, cadmium column reduction assay, ultraviolet spectroscopy and ion chromatography, require expensive equipment and tedious operation processes. Moreover, most of the methods involve the use of toxic and noxious reagents, which is easy to cause secondary pollution (Alahi and Mukhopadhyay, 2018). Some novel methods based on electrochemical technology can overcome these defects and realize the rapid detection of nitrate (Bui et al., 2016; Cosnier et al., 2008), but the problems of weak signal and electrode consumption remain unsolved. More importantly, the above methods cannot accomplish the dual detection of BOD and nitrate, which increases the cost and error of water monitoring to a certain extent.

Water quality monitoring based on electrochemical microbial biosensors might provide a solution to this limitation (Jiang et al., 2018). The sensing element of the biosensors is the electrochemically active bacteria (EAB), which can directly convert the chemical energy in organic matters into electrical energy by extracellular electron transfer (EET) process. Previous studies have demonstrated that the outward EET rate of EAB, *i.e.* output current, has a good linear relationship with organic matter concentration in a certain range; thus, tracking the current enables a rapid BOD measurement (Kim et al., 2003). On this basis, a series of studies were conducted to further optimize the EAB type (Yi et al., 2018), sensor configuration (Peixoto et al., 2011), control mode (Modin and Wilen, 2012) and operation parameters (Hsieh et al., 2016), improving the detection range and accuracy. Notably, nitrate can also be detected by measuring the output current of EAB. Since nitrate is a common electron acceptor of microbial metabolism, the presence of nitrate can compete with outward EET for electron, and thus decreases output current to some extent (Liu et al., 2014). Wang et al. (2018) investigated the correlation between the inhibition ratio of output current and nitrate; the results demonstrated a good linear relationship and developed a novel nitrate monitoring method. However, BOD measurement is based on the positive effect of biodegradable organic matters on EAB output current, whereas nitrate detection depends on the inhibitory effect of nitrate on the current (Srinivasan and Butler, 2017). Considering the coexistence of organic matters and nitrate in real water, how to achieve the dual detection of the two indicators remains unexplored.

In contrast with outward EET, an early study revealed that some EAB are capable of inward EET (Gregory et al., 2004), *i.e.* directly capturing electrons from an electrode to reduce soluble electron acceptors and maintain their metabolism. Nitrate is one of the soluble electron acceptors, and can be reduced to nitrogen by the EAB with inward EET capability (Gregoire et al., 2014; Pous et al., 2014). Besides, inward EET rate probably correlates with the concentration of extracellular nitrate. With the changes of nitrate, the inward current of EAB fluctuated and exhibited a similar trend (Pous et al., 2016); when nitrate was depleted, the inward current also decreased and almost dropped to 0 μA (Su et al., 2012). Therefore, nitrate detection may be available with the inward EET capacity of EAB. Moreover, the dual detection of BOD and nitrate in water might be achieved by using specific EAB capable of both inward and outward EET, *i.e.* bidirectional EET. However, only the application of bidirectional EET in wastewater treatment was recently revealed (Jiang and Zeng, 2019), and the potential application in water monitoring still needs further research.

The primary challenge is the limited knowledge of the EAB capable of organic oxidation by outward EET and nitrate reduction by inward EET. Some mixed cultures are confirmed with the ability of bidirectional EET (Liang et al., 2019; Pous et al., 2016). However, the complex microbial interaction and diverse metabolism in mixed culture are not conducive to the specificity of BOD and nitrate detection. Moreover, the evolution of microbial community structure and the corresponding changes of electrochemical characteristics limit the repeatability. Several model electricigens, such as *Geobacter sulfurreducens*, *Shewanella oneidensis* MR-1, have also been proved to catalyze bidirectional EET (Ross et al., 2011); but all shows a poor ability to reduce nitrate (Carpentier et al., 2005). Recently, *Shewanella loihica* PV-4, another model electricigen (Newton et al., 2009), is confirmed with the capability of bidirectional EET (Suo et al., 2019). Since *S. loihica* PV-4 is also a common denitrifying microorganism in sewage treatment (Yoon et al., 2015), its application in the dual detection of BOD and nitrate becomes possible. Therefore, this study firstly testified the bidirectional EET ability of *S. loihica* PV-4, and systematically investigated the differences between outward and inward EET processes. Then the feasibility of BOD measurement based on the outward EET of *S. loihica* PV-4 and nitrate detection based on the inward EET was explored. Finally, a novel method of the dual detection of BOD and nitrate using *S. loihica* PV-4 was established.

2. Materials and methods

2.1. BES construction and start up

Four identical three-electrode BESs (BES1-4) were constructed, and each BES contained a working electrode (WE), a counter electrode (CE) and a reference electrode (RE). WE was composed of a 2.5 cm × 2.5 cm piece of carbon cloth (WOS1009, CeTech, China), which was pretreated by acetone soaking and high-temperature heating (Yang et al., 2017b). The carbon cloth was fixed with an electrode clamp (J110, AiDa, China), resulting in an effective area of 5.8 cm^2. CE and RE were a platinum plate electrode (Pt210, AiDa, China) and a Ag/AgCl electrode (R0303, AiDa, China; 0.205 V *vs.* the standard hydrogen electrode), respectively. Each BES had a total volume of 50 mL and was sealed with a polytetrafluoroethylene lid with 5 holes, which were used for WE, CE, RE, inlet and outlet. All the components of the BESs except for Ag/AgCl electrodes were autoclaved prior to use. The Ag/AgCl electrodes were soaked overnight in 75% alcohol and sterilized with ultraviolet radiation (Sun et al., 2015).

BES1-4 were divided into two groups, including outward BESs (BES1-2) and inward BESs (BESs3-4). *S. loihica* PV-4 was activated overnight, centrifuged, resuspended in phosphate buffer, and then was used as inoculum. All the BESs were inoculated with the same inoculation ratio (30% v/v) in a laminar flow cabinet (SW-CJ-1F, Airtech, China). After inoculation, BES1-2 were fed with 25 mL outward electrolyte while the others were fed with 25 mL inward electrolyte. The outward electrolyte contained 1 g/L $NaHCO_3$, 0.13 g/L KCl, 0.027 g/L $CaCl_2{\cdot}2H_2O$, 0.2 g/L $MgCl_2{\cdot}6H_2O$, 5.85 g/L NaCl, 7.2 g/L HEPES, 1.12 g/L sodium lactate (NaLa) and 0.1 g/L yeast extract. The inward electrolyte was developed from the outward electrolyte by the removal of NaLa and yeast extract, but amended with 0.85 g/L $NaNO_3$ as the electron acceptor. During the start-up process, self-circulation was

operated at a flow rate of 3 mL/min (HRT = 15 min) to accelerate biofilm formation and enhance mass transfer (Gregoire et al., 2014). A potentiostat (CHI1030C, ChenHua, China) was used to maintain the potential of WE constant. Specifically, based on the results of pre-experiment, BES1-2 were poised at 0 V while BES3-4 were poised at −0.5 V. All the BESs were incubated at 22 ℃ and the currents were continuously recorded. Half of electrolyte was refreshed once BES current decreased below 30 μA. All potentials in this study are referred to Ag/AgCl electrode.

2.2. Electrochemical analysis: characterization of polarization reaction and EET process

All the BESs were electrochemically characterized after the start-up process. Polarization curve and electrochemical impedance spectroscopy (EIS) were measured to analyze the internal resistance of the BESs. Turnover cyclic voltammetry (CV) curves were recorded to investigate the onset potentials of organic oxidation and nitrate reduction under sufficient substrate condition. Non-turnover CV and differential pulse voltammetry (DPV) were conducted to reveal the redox properties of outward and inward EET processes without substrate.

Polarization curves were measured *via* linear sweep voltammetry. The applied potentials of outward BESs increased from open-circuit potential (OCP) to 0.4 V with a scan rate of 0.3 mV/s, while the potentials of inward BESs were from OCP to −0.6 V with the same scan rate. The terminal potentials (0.4 V and −0.6 V) have been optimized to avoid obvious oxygen/hydrogen evolution reactions. EIS was conducted with a frequency range of 10 mHz ~ 100 kHz and a signal amplitude of 10 mV (Yi et al., 2019). Turnover and non-turnover CV curves were performed from −0.6 V to 0.4 V with the following parameters: scan rate of 10.0 mV/s, holding time of 30 s, and 3 cycles. DPV was conducted with the same potential scan range, and the other parameters were as follows: pulse height of 50 mV, pulse width of 100 ms, step height of 1 mV and step time of 1 s.

2.3. Single detection tests of BOD and nitrate

Based on the respective outward EET and inward EET, BES1-2 and BES3-4 were used for the single detection tests of BOD and nitrate by *S. loihica* PV-4. Firstly, while stable operation, all the BESs were fed with the fresh electrolyte without substrate to analyze the substrate dependency of outward and inward EET. Then, the BESs were operated with different electrolytes containing specific concentrations of substrate and the currents were recorded. Finally, regression analyses and biometric modelling were used to investigate the relationship between outward current and BOD as well as the relationship between inward current and nitrate. Before each test, the currents of all the BESs were confirmed to decrease below 20 μA to ensure the same initial condition. BES1-2 were tested with outward electrolytes containing 1 mM, 2 mM, 3 mM, 5 mM and 10 mM NaLa, respectively. According to the international standard method of BOD measurement, the BOD of the outward electrolyte containing 1 mM NaLa was 43.5 mg/L; thus, the tested BOD concentrations ranged from 43.5 mg/L to 435 mg/L. Similarly, BES3-4 were sequentially operated with inward electrolytes containing 0.05 mM, 0.125 mM, 0.25 mM, 0.375 mM and 0.5 mM $NaNO_3$, respectively, resulting in a NO_3^--N concentration range of 0.7–7 mg/L. During all the tests, the applied potentials of BES1-2 were maintained at 0 V while the potentials of BES3-4 were −0.5 V. Besides, all the electrolytes were purged with N_2 to avoid the interference of oxygen.

2.4. Dual detection tests of BOD and nitrate

After the single detection, all the BESs were alternately fed with outward and inward electrolytes to acclimate bidirectional EET ability (Cheng et al., 2012). Then, the BESs were operated with a potential step and were loaded with the electrolytes containing both NaLa and nitrate; both the outward and inward currents were recorded to testify the feasibility of the dual detection of BOD and nitrate. The applied potentials included 0 V and −0.5 V, and each potential lasted for 30 min. Two different ratios of NaLa and nitrate (3 mM/0.25 mM and 0.5 mM/0.5 mM) were used to simulate the varied C/N ratio of real water. The prediction of BOD and nitrate was calculated by using the biometric models derived from the single BOD and nitrate detection.

2.5. Analysis and calculation

The peaks in CV and DPV curves were detected using the first derivative function of Prism 8.2 (GraphPad Software Inc., USA). The midterm potential of redox couples was defined as the average of oxidative and reductive peak potentials. The relationship between BES current and substrate concentration was fitted by the combination of linear and Michaelis-Menten models *via* Prism 8.2. EIS spectrum was fitted with an equivalent circuit (R_s + CPE/R_p) *via* Zman (WonATech Co., Korea), where R_s and R_p account for ohmic resistance and polarization resistance, respectively, CPE is a double-layer capacitor (Wu et al., 2014).

3. Results and discussion

3.1. Bidirectional EET performance of S. loihica PV-4

The current evolution of outward and inward BESs during the start-up process is shown in Fig. 1a. As expected, the outward BESs generated obvious currents after a short lag period, and the currents reached a peak of ~30 μA in the first cycle, confirming the outward EET ability of *S. loihica* PV-4 (Newton et al., 2009). As for the inward BESs, it was notable that the inward currents changed with a similar trend and the maximum of inward currents in the first cycle was about −110 μA. These results revealed that *S. loihica* PV-4 can directly uptake electrons from a solid electrode and is capable of bidirectional EET. As the enrichment of biofilm, both the outward and inward currents gradually increased but showed different characteristics. Compared to the outward BESs, the inward BESs exhibited shorter start-up time but a lower electron transfer rate. As shown in Fig. 1a, the maximum currents of inward BESs became stable from the fourth cycle while that of outward BESs stabilized after seven cycles. After the start-up, the maximum inward current (~190 μA) was only 36.6% of the maximum outward current (~520 μA). Correspondingly, the double-layer capacitance of outward BESs was obviously higher than that of inward BESs (Fig. 1e), indicating higher polarizability and more residual charges in the outward EET process. Moreover, the current evolution in a single cycle was distinct between the outward and inward BESs. Specifically, after the refreshment of electrolyte, the outward current rapidly increased to peak and then dropped below 30 μA while the inward current remained nearly unchanged. This phenomenon was similar to the results in a recent bidirectional EET study based on *Alcaligenes faecalis* (Yu et al., 2018), which might be due to that both biofilm and suspended biomass contributed to outward current (Newton et al., 2009) while only biofilm was responsible for inward current (Strycharz et al., 2008).

The internal resistance of polarization reaction and its composition were also characterized. As shown in Fig. 1b-c, by calculating the slope of the polarization curves (Liang et al., 2007), it was revealed that the outward and inward BESs had similar total resistance (~750 Ω). Similar results were also obtained from EIS analysis (Fig. 1d), and the polarization resistance of outward and inward BESs was 874.0 ± 19.5 Ω and 823.4 ± 67.5 Ω, respectively. Previous studies have reported that some bidirectional EET EAB (*e.g. Shewanella oneidensis* and *Geobacter soil*) showed obviously different polarization resistance between inward and outward EET pathways (Okamoto et al., 2014; Yang et al., 2017a). In this study, similar polarizing capabilities were observed under outward and inward EET conditions, indicating *S. loihica* PV-4 is more suitable for the study of bidirectional EET mechanism.

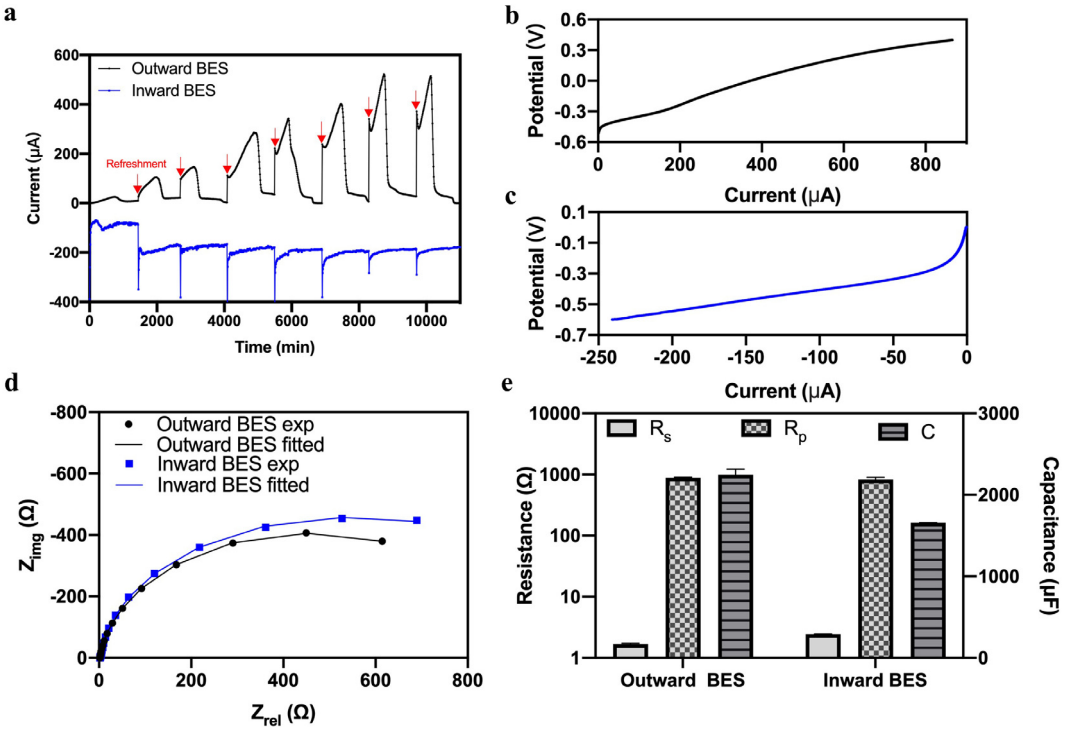

Fig. 1. Bidirectional EET performance of *S. loihica* PV-4: (a) current evolution in the start-up process; (b) polarization curve of the outward BES; (c) polarization curve of the inward BES; (d) EIS spectra; (e) composition of the internal resistance.

3.2. Polarization characteristics and redox properties of bidirectional EET process

The polarization characteristics of outward and inward BESs were revealed by turnover CV (Fig. 2a and 2c). The CVs of outward BESs showed a positive S-shape while a negative S-shape was observed in the CVs of inward BESs; this difference is due to the distinct characteristics of anodic and cathodic polarization (Pous et al., 2016). Besides, based on the CVs of outward BESs, the oxidative currents largely increased at the potentials above −0.47 V, which was similar to the reported onset potential of NaLa oxidation catalyzed by *Shewanella* (Bretschger et al., 2010). Two redox couples, $E_{o,1}$ (−0.41 V) and $E_{o,2}$ (0.17 V), were identified from the first derivative (Fig. 2b), indicating the diverse metabolic pathways of *Shewanella* at different potentials (Jain et al.,

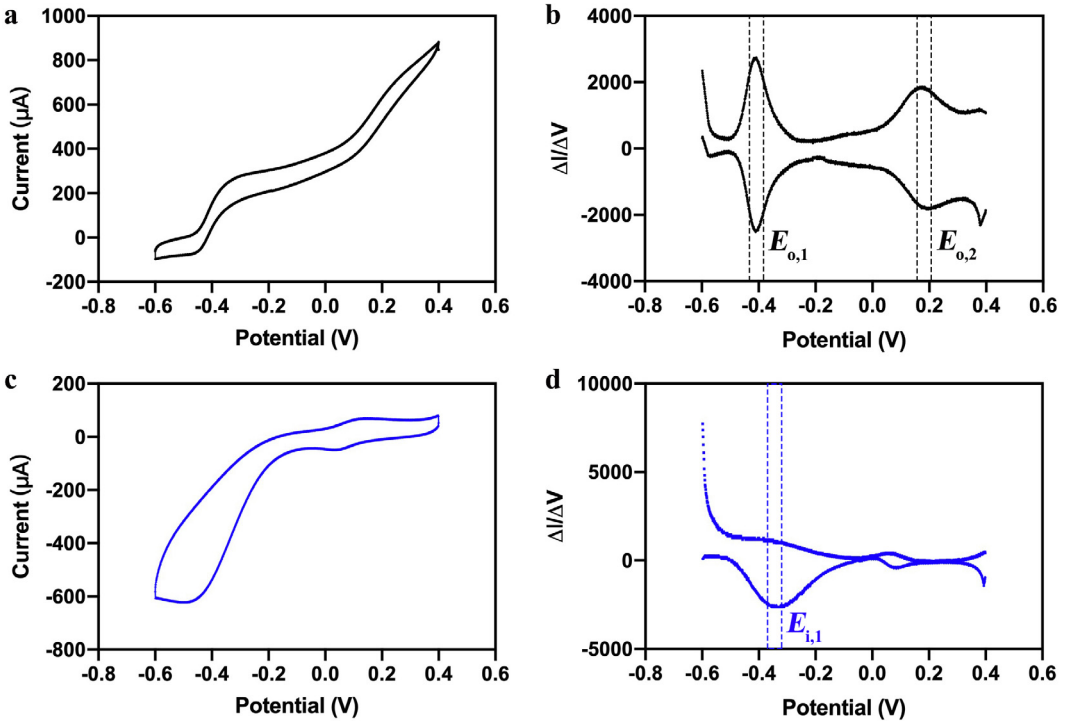

Fig. 2. Turnover CVs and the corresponding first derivative curves of the outward BES (a-b) and inward BES (c-d).

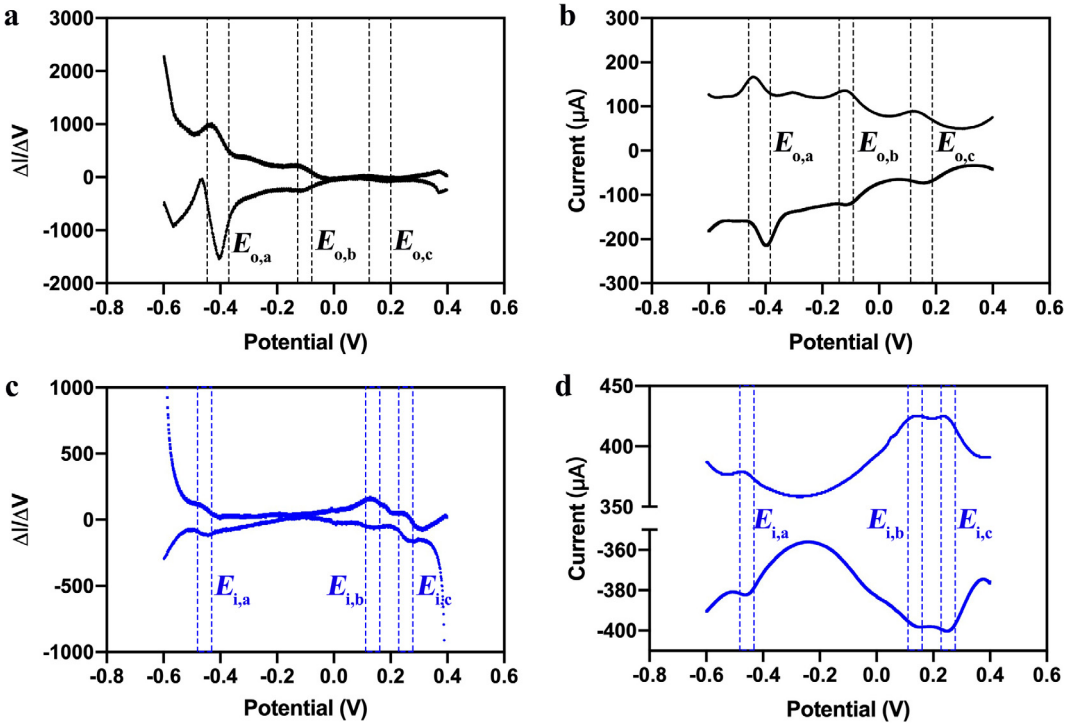

Fig. 3. First derivative curves of non-turnover CV and DPV curves of the outward BES (a-b) and inward BES (c-d).

2012; Hirose et al., 2018; Pinto et al., 2018). As for the CVs of inward BESs, the reductive current occurred at the potentials below −0.1 V (Fig. 2c), which was close to the revealed onset potential (-0.125 V) of nitrate reduction (Gregoire et al., 2014). Only one redox couple ($E_{i,1}$) at −0.32 V was obtained from the first derivative (Fig. 2d), which represents the half-wave potential of nitrate reduction (Pous et al., 2016; Pous et al., 2014).

The bidirectional EET mechanism of *S. loihica* PV-4 was investigated by the combination of non-turnover CV and DPV. Three redox couples ($E_{o,a}$, $E_{o,b}$, $E_{o,c}$) were obtained from the outward BESs (Fig. 3a-b). The mid-term potential of $E_{o,a}$ was −0.43 V, which was also observed in a previous study (Jain et al., 2012) and might be related to the indirect EET *via* self-secreted riboflavin (Carmona-Martinez et al., 2013). The mid-term potential of another redox couple $E_{o,b}$ (−0.12 V) was similar with that of *OmcA* (−0.119 V, Field et al., 2000), indicating the possible co-existence of direct EET (Yu et al., 2015). Moreover, an unreported redox couple $E_{o,c}$ (0.14 V) was also observed, which might related to the metabolism of *S. loihica* PV-4 at relatively high potentials. As for the inward BESs, three redox couples ($E_{i,a}$, $E_{i,b}$, $E_{i,c}$) were identified as well (Fig. 3c-d). Interestingly, it was noted that the mid-term potentials of $E_{i,a}$ (−0.460 V) and $E_{i,b}$ (0.145 V) were close to those of $E_{o,a}$ and $E_{o,c}$, which indicated that the outward and inward EET pathways of *S. loihica* PV-4 might share several electron transport components (Ross et al., 2011; Strycharz et al., 2011; Pous et al., 2016). Due to the limited research of *S. loihica* PV-4 inward EET, the specific functions of these components still need further study.

3.3. Single detection of BOD and nitrate

By conducting substrate dependency test, it was noted that the currents of both inward and outward BESs decreased to 0 μA within 6 h after the refreshment of electrolyte, confirming the dependency of inward current on organic matter as well as the dependency of outward current on nitrate. Notably, the currents of inward BESs decreased more slowly than those of outward BESs. Similar results were also obtained in a previous study (Gregoire et al., 2014), and this phenomenon might be attributed to the residual nitrate after refreshment and the relatively poor nitrate reduction rate (~0.53 NO_3^--N mg·cm^{-2}·d^{-1}) of inward BESs.

The responses of outward current to BOD were shown in Fig. 4c. With the increase of organic matter, the maximum current, total coulomb yield and cycle length all increased. These indicators have been verified to be well correlated with BOD (Hsieh et al., 2016; Jiang et al., 2017; Kim et al., 2003). To shorten the detection time, the maximum outward current (I_p, μA) was selected as the indicator of outward BES performance. Notably, I_p showed a good linear relationship with BOD concentration in a relatively low range (from 0 mg/L to 130.5 mg/L) (Wang et al., 2019). However, with the further increase of BOD, I_p increased at a much slower rate (Wang et al., 2019), which presented a similar trend of Michaelis-Menten kinetics. Thus, the relationship between I_p and BOD concentration (mg/L) was fitted using both linear model and Michaelis–Menten model as follows (Fig. 4e):

$$I_p = 1.467BOD + 144.5 (0 \leqslant BOD \leqslant 130.5,\ R^2 = 0.991) \quad (1)$$

$$I_p = 610.5/(BOD + 163.8) (0 \leqslant BOD \leqslant 435.0,\ R^2 = 0.987) \quad (2)$$

Both the determination coefficients (R^2) were above 0.98, indicating that the fitted models were able to express > 98% of the variability in I_p. Many previous studies have reported the linear relationship between EAB current and BOD. However, based on a single linear model, the upper detection limit of BOD was generally less than 300 mg/L and remained to be improved (Kim et al., 2003; Jiang et al., 2017; Wang et al., 2019). In this study, the combination of linear model and Michaelis–Menten model not only ensures the accuracy of BOD detection, but also increases the detection range. Besides, it was notable that the outward currents can rapidly reach the peak (< 1 h) in all the tests, which is much shorter than the reported detection time of 4–10 h (Modin and Wilen, 2012; Hsieh et al., 2016; Wang et al., 2019), indicating the good outward EET performance of *S. loihica* PV-4 and its feasibility for BOD detection.

Similar to BOD detection, the maximum inward current (I_o, μA) increased with the increase of nitrate concentration (*Nir*, mg/L) (Fig. 4d). The relationship between I_o and *Nir* was analyzed *via* similar methods as above (Fig. 4f), and the fitted models are shown as

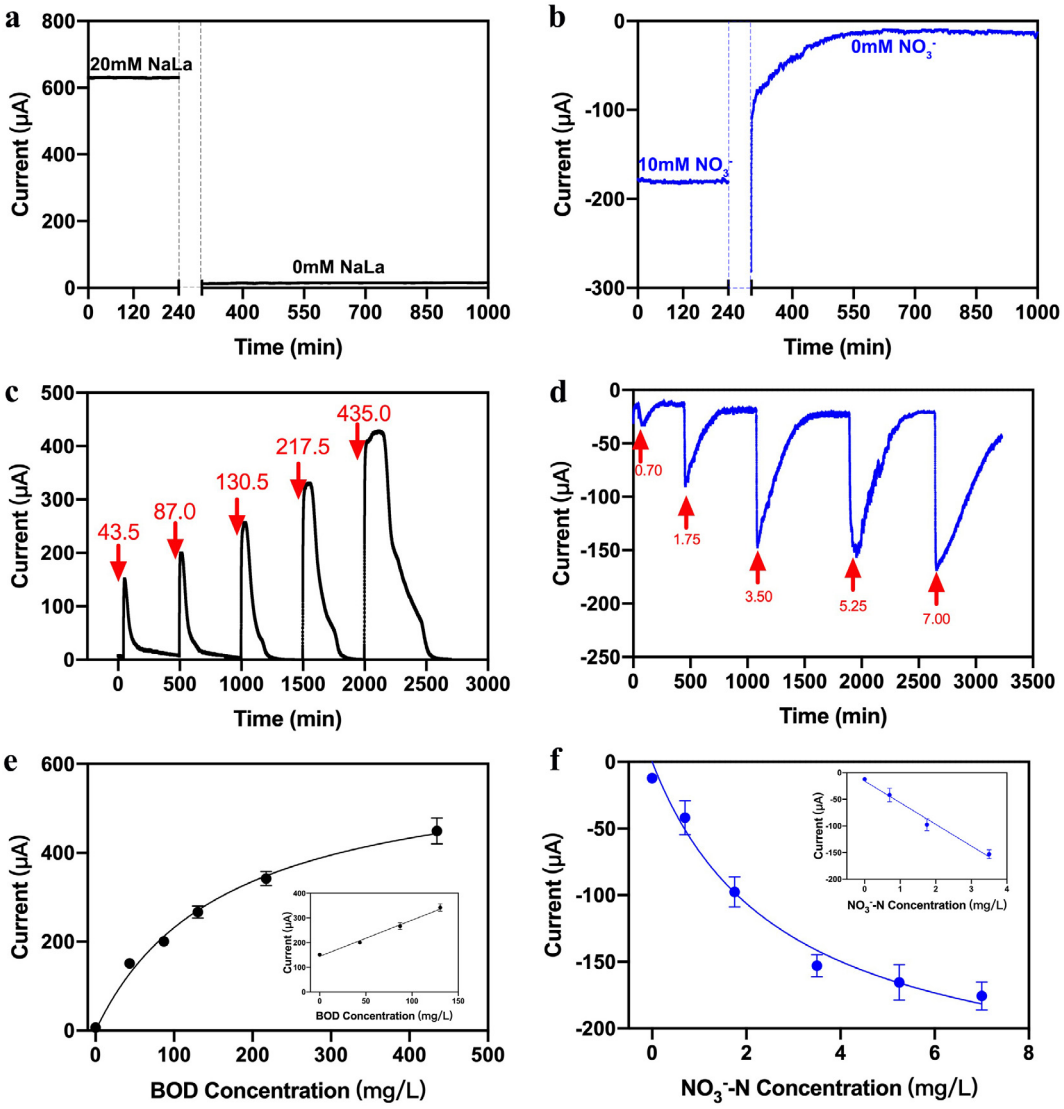

Fig. 4. Single detection of BOD and nitrate using *S. loihica* PV-4 BESs: (a) dependency of *S. loihica* PV-4 outward EET on organic matter; (b) dependency of *S. loihica* PV-4 inward EET on nitrate; (c) responses of the outward current to BOD; (d) responses of the inward current to nitrate; (e) relationship between the maximum outward current and BOD; (f) relationship between the maximum inward current and nitrate.

equations (III)-(IV):

$$I_o = -15.76Nir - 40.62 \ (0 \leqslant Nir \leqslant 3.5, \ R^2 = 0.986) \quad (3)$$

$$I_o = {}^{-253.4}/_{(Nir + 2.772)} \ (0 \leqslant Nir \leqslant 7.0, \ R^2 = 0.969) \quad (4)$$

R^2 of each model was more than 0.96 and it indicated that > 96% variability in I_o can be explained by *Nir*, which proved for the first time the feasibility of nitrate detection by inward BES. Compared with the nitrate monitoring by outward EET (Wang et al., 2018), faster response time (< 30 min) and a lower detection limit (0.75 NO_3^--N mg/L) were obtained in this study, suggesting the enhanced performance of nitrate detection by inward EET. Besides, the sensitivity of nitrate detection achieved 15.76 μA/mg in the linear range, which is obviously higher than the reported sensitivity (< 1 μA/mg) based on immobilized nitrate reductase (Can et al., 2012; Cosnier et al., 2008). Moreover, with the biofilm as sensing element, the inward BES is capable of self-sustainability, which make it more suitable for nitrate detection.

3.4. Simultaneous detection of BOD and nitrate

The single detection of BOD and nitrate by *S. loihica* PV-4 was based on the anodic polarization (oxidation reaction) and cathodic polarization (reduction reaction), respectively (Section 3.3). However, anodic and cathodic polarization may occur simultaneously with the coexistence of organic matter and nitrate, which probably deteriorates the detection specificity. Based on electrode kinetics, the degree of polarization is regulated by the applied potential. Since the onset potentials of NaLa oxidation and nitrate reduction were respective −0.47 V and −0.1 V, it was speculated that only anodic or cathodic polarization can occur on electrode surface at the potential of 0 V or −0.5 V. This hypothesis was further confirmed by the response of the BES currents to the potential step (Fig. 5). Thus, with the exclusive anodic/cathodic polarization, the dual detection of BOD and nitrate can be achieved by successively using the outward and inward EET processes of *S. loihica* PV-4 *via* potential regulation.

After acclimation by periodic polarity reversal (Cheng et al., 2012), all the BESs were fed with the electrolytes containing different ratios of NaLa and nitrate. As shown in Fig. 6, with the applied potential step, the BESs exhibited alternative electron generation and uptake, indicating a new characteristic of ano-cathodophilic capability of *S. loihica* PV-4 biofilm. Notably, when BOD and NO_3^--N concentrations were respective 130.5 mg/L and 3.5 mg/L, the BESs presented a high

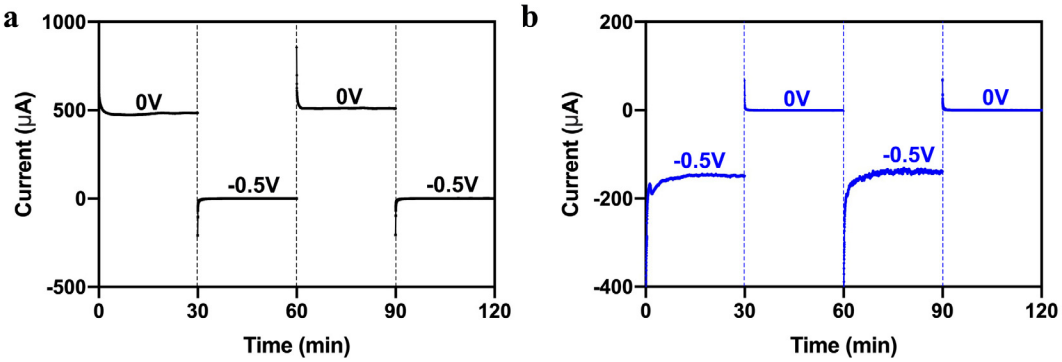

Fig. 5. Current responses of the outward BES (a) and inward BES (b) to the potential step.

outward current (243.3 ± 25.2 μA) and a low inward current (−134.3 ± 17.1 μA). However, as BOD decreased to 21.8 mg/L and NO_3^--N increased to 7.0 mg/L, enhanced inward EET (−177.0 ± 7.1 μA) and suppressive outward EET (65.3 ± 12.8 μA) were observed. By using the fitted models (equations I-IV) in section 3.3, the predicted values of BOD and NO_3^--N are displayed in Table 1. The relative errors were all lower than 20%, indicating the feasibility of the dual detection of BOD and nitrate using *S. loihica* PV-4.

However, considering the natural microorganisms and complex composition in real water, there are still several challenging problems to be solved before the practical application of *S. loihica* PV-4 BES. The primary problem is the threat of microbial pollution to the pure culture of *S. loihica* PV-4. An efficient solution is the pretreatment and sterilization of water sample, which can be achieved by using strainer together with fine filtration through 0.22 μm pore size membrane. Periodic bioaugmentation is also suggested to maintain a high abundance of *S. loihica* PV-4 in biofilm and ensure the accuracy of detection. Besides, some common pollutants in water, *e.g.* nitrite, can also serve as the electron acceptors of *S. loihica* PV-4 inward EET, which probably decreases the specificity of nitrate detection. According to a previous study, the onset potential of nitrite reduction is lower than that of nitrate reduction (Pous et al., 2014), therefore the interfere caused by nitrite and other electron acceptors might be eliminate by the optimization of applied potential. In addition, the exclusive nitrate reduction of *S. loihica* PV-4 can also be realized by changing the metabolism pathway with genetic mutations. Besides its application in water monitoring, the bidirectional EET of *S. loihica* PV-4 also holds great prospects for simultaneous removal of nitrogen and carbon, pollutants mineralization, and energy conservation (Jiang and Zeng, 2019). Further works are eagerly required to enlarge its application and reveal the mechanism of *S. loihica* PV-4 bidirectional EET.

4. Conclusions

This study investigated the bidirectional EET of *S. loihica* PV-4 and its application in water monitoring. The results revealed that the outward EET was correlated with BOD ($R^2 > 0.98$), whereas the inward EET was associated with nitrate ($R^2 > 0.96$); thus, a novel nitrate detection method based on inward EET was proposed. Besides, based on the bidirectional EET of *S. loihica* PV-4, the dual detection of BOD and nitrate was achieved for the first time and was characterized by fast analysis and high accuracy.

Table 1
Relative errors of the dual detection for BOD and nitrate by *S. loihica* PV-4 BESs.

Sample		Amount added	Test results	Relative error
Electrolyte with high C/N ratio	BOD	130.5	109.5 ± 18.9	17.20%
	NO_3^--N	3.5	3.3 ± 0.8	19.30%
Electrolyte with low C/N ratio	BOD	21.8	19.7 ± 4.3	15.70%
	NO_3^--N	7.0	6.5 ± 0.9	11.80%

CRediT authorship contribution statement

Yue Yi: Conceptualization, Methodology, Investigation, Validation, Visualization, Writing - original draft. **Ting Zhao:** Formal analysis, Writing - review & editing. **Beizhen Xie:** Visualization, Methodology. **Yuxuan Zang:** Investigation. **Hong Liu:** Conceptualization, Supervision.

Declaration of Competing Interest

The authors declare that they have no known competing financial interests or personal relationships that could have appeared to influence the work reported in this paper.

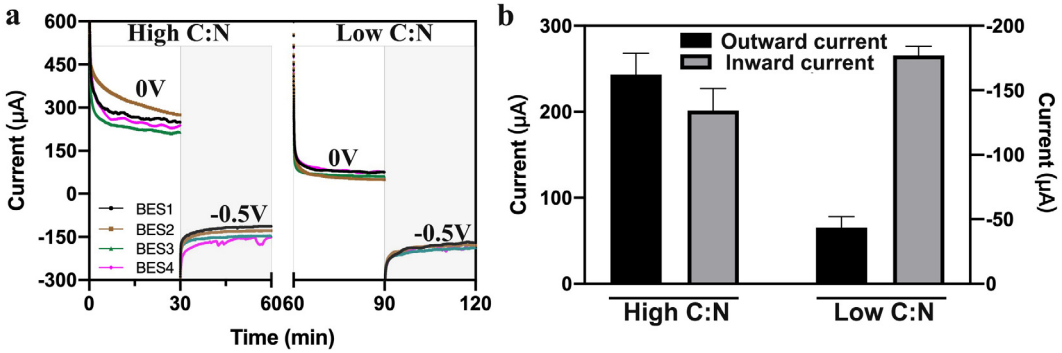

Fig. 6. Current responses of *S. loihica* PV-4 BESs to electrolytes with different C:N ratios.

Acknowledgements

This work was financially supported by grants from the National Natural Science Foundation of China [31770135] and the Fundamental Research Funds for the Central Universities.

Appendix A. Supplementary data

Supplementary data to this article can be found online at https://doi.org/10.1016/j.biortech.2020.123402.

References

Alahi, M.E.E., Mukhopadhyay, S.C., 2018. Detection methods of nitrate in water: a review. Sens. Actuators A-Phys. 280, 210–221.
Bretschger, O., Cheung, A.C.M., Mansfeld, F., Nealson, K.H., 2010. Comparative microbial fuel cell evaluations *of Shewanella* spp. Electroanal. 22 (7–8), 883–894.
Bui, M.P.N., Brockgreitens, J., Ahmed, S., Abbas, A., 2016. Dual detection of nitrate and mercury in water using disposable electrochemical sensors. Biosens. Bioelectron. 85, 280–286.
Can, F., Ozoner, S.K., Ergenekon, P., Erhan, E., 2012. Amperometric nitrate biosensor based on carbon nanotube/polypyrrole/nitrate reductase biofilm electrode. Mat. Sci. Eng. C-Mater. 32 (1), 18–23.
Carey, D.E., Yang, Y., McNamara, P.J., Mayer, B.K., 2016. Recovery of agricultural nutrients from biorefineries. Bioresour. Technol. 215, 186–198.
Carmona-Martinez, A.A., Harnisch, F., Kuhlicke, U., Neu, T.R., Schroeder, U., 2013. Electron transfer and biofilm formation of *Shewanella putrefaciens* as function of anode potential. Bioelectrochemistry 93, 23–29.
Carpentier, W., De Smet, L., Van Beeumen, J., Brige, A., 2005. Respiration and growth of *Shewanella oneidensis* MR-1 using vanadate as the sole electron acceptor. J. Bacteriol. 187 (10), 3293–3301.
Cheng, K.Y., Ginige, M.P., Kaksonen, A.H., 2012. Ano-cathodophilic biofilm catalyzes both anodic carbon oxidation and cathodic denitrification. Environ. Sci. Technol. 46 (18), 10372–10378.
Cosnier, S., Da Silva, S., Shan, D., Gorgy, K., 2008. Electrochemical nitrate biosensor based on poly (pyrrole–viologen) film–nitrate reductase–clay composite. Bioelectrochemistry 74 (1), 47–51.
Field, S.J., Dobbin, P.S., Cheesman, M.R., Watmough, N.J., Thomson, A.J., Richardson, D.J., 2000. Purification and magneto-optical spectroscopic characterization of cytoplasmic membrane and outer membrane multiheme c-type cytochromes from *Shewanella frigidimarina* NCIMB400. J. Biol. Chem. 275 (12), 8515–8522.
Gregoire, K.P., Glaven, S.M., Hervey, J., Lin, B.C., Tender, L.M., 2014. Enrichment of a high-current density denitrifying microbial biocathode. J. Electrochem. Soc. 161 (13), 3049–3057.
Gregory, K.B., Bond, D.R., Lovley, D.R., 2004. Graphite electrode as electron donors for anaerobic respiration. Environ. Microbiol. 6, 596–604.
Hirose, A., Kasai, T., Aoki, M., Umemura, T., Watanabe, K., Kouzuma, A., 2018. Electrochemically active bacteria sense electrode potentials for regulating catabolic pathways. Nat. Commun. 9 (1), 1083.
Hsieh, M.C., Cheng, C.Y., Liu, M.H., Chung, Y.C., 2016. Effects of operating parameters on measurements of biochemical oxygen demand using a mediatorless microbial fuel cell biosensor. Sensors-Basel. 16 (1), 35–44.
Hu, H.D., Ren, H.Q., 2019. Removal of bioavailable dissolved organic nitrogen in wastewater by membrane bioreactors as posttreatment: implications for eutrophication control. Bioresour. Technol. 271, 496–499.
Jain, A., Zhang, X.M., Pastorella, G., Connolly, J.O., Barry, N., Woolley, R., Krishnamurthy, S., Marsili, E., 2012. Electron transfer mechanism in *Shewanella loihica* PV-4 biofilms formed at graphite electrode. Bioelectrochemistry. 87, 28–32.
Jiang, Y., Liang, P., Liu, P.P., Miao, B., Bian, Y.H., Zhang, H.L., Huang, X., 2017. Enhancement of the sensitivity of a microbial fuel cell sensor by transient-state operation. Environ. Sci.-Wat. Res. 3, 472–479.
Jiang, Y., Yang, X.F., Liang, P., Liu, P.P., Huang, X., 2018. Microbial fuel cell sensors for water quality early warning systems: fundamentals, signal resolution, optimization and future challenges. Renew. Sust. Energ. Rev. 81, 292–305.
Jiang, Y., Zeng, R.J., 2019. Bidirectional extracellular electron transfers of electrode-biofilm: Mechanism and application. Bioresour. Technol. 271, 439–448.
Jouanneau, S., Recoules, L., Durand, M.J., Boukabache, A., Picot, V., Primault, Y., Lakel, A., Sengelin, M., Barillon, B., Thouand, G., 2014. Methods for assessing biochemical oxygen demand (BOD): A review. Water Res. 49, 62–82.
Kim, B.H., Chang, I.S., Gil, G.C., Park, H.S., Kim, H.J., 2003. Novel BOD (biological oxygen demand) sensor using mediator-less microbial fuel cell. Biotechnol. Lett. 25 (7), 541–545.
Liang, D.D., He, W.H., Li, C., Yu, Y.L., Zhang, Z.H., Ren, N.Q., Feng, Y.J., 2019. Bidirectional electron transfer biofilm assisted complete bioelectrochemical denitrification process. Chem. Eng. J. 375, 121960.
Liang, P., Huang, X., Fan, M.Z., Cao, X.X., Wang, C., 2007. Composition and distribution of internal resistance in three types of microbial fuel cells. Appl. Microbiol. Biot. 77 (3), 551–558.
Liu, B.C., Lei, Y., Li, B.K., 2014. A batch-mode cube microbial fuel cell based “shock” biosensor for wastewater quality monitoring. Biosens. Bioelectron. 62, 308–314.
Liu, L., Zhai, J.F., Zhu, C.Z., Gao, Y., Wang, Y., Han, Y.C., Dong, S.J., 2015. One-pot synthesis of 3-dimensional reduced graphene oxide-based hydrogel as support for microbe immobilization and BOD biosensor preparation. Biosens. Bioelectron. 63, 483–489.
Modin, O., Wilen, B.M., 2012. A novel bioelectrochemical BOD sensor operating with voltage input. Water Res. 46 (18), 6113–6120.
Newton, G.J., Mori, S., Nakamura, R., Hashimoto, K., Watanabe, K., 2009. Analyses of current-generating mechanisms of *Shewanella loihica* PV-4 and *Shewanella oneidensis* MR-1 in microbial fuel cells. Appl. Environ. Microb. 75 (24), 7674–7681.
Okamoto, A., Hashimoto, K., Nealson, K.H., 2014. Flavin redox bifurcation as a mechanism for controlling the direction of electron flow during extracellular electron transfer. Angew. Chem. 126 (41), 11168–11171.
Peixoto, L., Min, B., Martins, G., Brito, A.G., Kroff, P., Parpot, P., Angelidaki, I., Nogueira, R., 2011. In situ microbial fuel cell-based biosensor for organic carbon. Bioelectrochemistry 81 (2), 99–103.
Pinto, D., Coradin, T., Laberty-Robert, C., 2018. Effect of anode polarization on biofilm formation and electron transfer in *Shewanella oneidensis*/graphite felt microbial fuel cells. Bioelectrochemistry 120, 1–9.
Pous, N., Carmona-Martínez, A.A., Vilajeliu-Pons, A., Fiset, E., Baneras, L., Trably, E., Dolors Balaguer, M., Colprim, J., Bernet, N., Puig, S., 2016. Bidirectional microbial electron transfer: Switching an acetate oxidizing biofilm to nitrate reducing conditions. Biosens. Bioelectron. 75, 352–358.
Pous, N., Koch, C., Colprim, J., Puig, S., Harnisch, F., 2014. Extracellular electron transfer of biocathodes: revealing the potentials for nitrate and nitrite reduction of denitrifying microbiomes dominated by *Thiobacillus* sp. Electrochem. Commun. 49, 93–97.
Ross, D.E., Flynn, J.M., Baron, D.B., Gralnick, J.A., Bond, D.R., 2011. Towards electrosynthesis in *shewanella*: energetics of reversing the mtr pathway for reductive metabolism. PloS One 6 (2), e16649.
Srinivasan, V.N., Butler, C.S., 2017. Ecological and transcriptional responses of anode-respiring communities to nitrate in a microbial fuel cell. Environ. Sci. Technol. 51 (9), 5334–5342.
Strycharz, S.M., Glaven, R.H., Coppi, M.V., Gannon, S.M., Perpetua, L.A., Liu, A., Nevin, K.P., Lovley, D.R., 2011. Gene expression and deletion analysis of mechanisms for electron transfer from electrodes to *Geobacter sulfurreducens*. Bioelectrochemistry. 80 (2), 142–150.
Strycharz, S.M., Woodard, T.L., Johnson, J.P., Nevin, K.P., Sanford, R.A., Loeffler, F.E., Lovley, D.R., 2008. Graphite electrode as a sole electron donor for reductive dechlorination of tetrachlorethene by *Geobacter lovleyi*. Appl. Environ. Microb. 74 (19), 5943–5947.
Su, W.T., Zhang, L.X., Li, D.P., Zhan, G.Q., Qian, J.W., Tao, Y., 2012. Dissimilatory nitrate reduction by *Pseudomonas alcaliphila* with an electrode as the sole electron donor. Biotechnol. Bioeng. 109 (11), 2904–2910.
Sun, D., Cheng, S.A., Wang, A.J., Li, F.J., Logan, B.E., Cen, K.F., 2015. Temporal-spatial changes in viabilities and electrochemical properties of anode biofilms. Environ. Sci. Technol. 49 (8), 5227–5235.
Suo, D., Fang, Z., Yu, Y.Y., Yong, Y.C., 2019. Synthetic curli enables efficient microbial electrocatalysis with stainless-steel electrode. AIChE J., e16897.
Wang, D.L., Liang, P., Jiang, Y., Liu, P.P., Miao, B., Hao, W., Huang, X., 2018. Open external circuit for microbial fuel cell sensor to monitor the nitrate in aquatic environment. Biosens. Bioelectron. 111, 97–101.
Wang, S.Q., Tian, S., Zhang, P.Y., Ye, J.P., Tao, X., Li, F., Zhou, Z.Y., Nabi, M., 2019. Enhancement of biological oxygen demand detection with a microbial fuel cell using potassium permanganate as cathodic electron acceptor. J. Environ. Manage. 252, 109682.
Wu, B.G., Feng, C.H., Huang, L.Q., Lv, Z.S., Xie, D.H., Wei, C.H., 2014. Anode-biofilm electron transfer behavior and wastewater treatment under different operational modes of bioelectrochemical system. Bioresour. Technol. 157, 305–309.
Yang, G.Q., Huang, L.Y., You, L.X., Zhuang, L., Zhou, S.G., 2017a. Electrochemical and spectroscopic insights into the mechanisms of bidirectional microbe-electrode electron transfer in *Geobacter soli* biofilms. Electrochem. Commun. 77, 93–97.
Yang, Q., Liang, S.N., Liu, J., Lv, J.W., Feng, Y.J., 2017b. Analysis of anodes of microbial fuel cells when carbon brushes are preheated at different temperatures. Catalysts 7 (11), 312.
Yi, Y., Xie, B.Z., Zhao, T., Liu, H., 2018. Comparative analysis of microbial fuel cell based biosensors developed with a mixed culture and *Shewanella loihica* PV-4 and underlying biological mechanism. Bioresour. Technol. 265, 415–421.
Yi, Y., Xie, B.Z., Zhao, T., Qian, Z.N., Liu, H., 2019. Effect of control mode on the sensitivity of a microbial fuel cell biosensor with *Shewanella loihica* PV-4 and the underlying bioelectrochemical mechanism. Bioelectrochemistry 128, 109–117.
Yoon, S., Sanford, R.A., Loeffler, F.E., 2015. Nitrite control over dissimilatory nitrate/nitrite reduction pathways in *Shewanella loihica* strain PV-4. Appl. Environ. Microb. 81 (10), 3510–3517.
Yu, L.P., Yuan, Y., Rensing, C., Zhou, S.G., 2018. Combined spectroelectrochemical and proteomic characterizations of bidirectional Alcaligenes faecalis-electrode electron transfer. Biosens. Bioelectron. 106, 21–28.
Yu, Y.Y., Guo, C.X., Yong, Y.C., Li, C.M., Song, H., 2015. Nitrogen doped carbon nanoparticles enhanced extracellular electron transfer for high-performance microbial fuel cells anode. Chemosphere 140, 26–33.
Zaitseva, A.S., Arlyapov, V.A., Yudina, N.Y., Alferov, S.V., Reshetilov, A.N., 2017. Use of one- and two-mediator systems for developing a BOD biosensor based on the yeast *Debaryomyces hansenii*. Enzyme Microb. Tech. 98, 43–51.